Journal of Ceramic Processing Research. Vol. 16, No. 3, pp. 287~290 (2015)

J O U R N A L O F
Ceramic Processing Research

Preparation and characterization of plasma-sprayed nanostructured- merwinite coating on Ti-6Al-4V

Mohammadreza Hadipour[a], Masoud Hafezi[b,c,*] and Saeed Hesaraki[b]

[a]*Department of Biomaterials, Science and Research Branch, Islamic Azad University, Yazd, Iran*
[b]*Biomaterials Group, Nanotechnology and Advanced Materials Department, Materials and Energy Research Center, Alborz, Iran*
[c]*Department of Biomedical Engineering, Faculty of Engineering, University of Malaya, Kuala Lumpur, Malaysia.*

In the present study, synthesized nanostructured merwinite ($Ca_3MgSi_2O_8$) bioactive coatings were successfully prepared by plasma-spray coating method. The phase composition and microstructure of the powders were examined by X-ray diffraction, scanning electron microscopy and transmission electron microscopy. Also the properties of the prepared coating were evaluated using XRD, AFM, SEM coupled with Energy-Dispersive X-ray analaysis and micro hardness analysis. XRD analysis indicated pure merwinite coatings were obtained. A uniform structure of the merwinite coating was found across the Ti-6Al-4V surface, with a thickness and surface roughness of the coating of about 16 and 0.252 + –0.02 μm, respectively. The results indicated that merwinite coating was obtained with a uniform and dense microstructure at the interface of the Ti-6A l-4V surface. Taken together, the results obtained indicated that plasma sprayed merwinite coating may be a candidate for orthopedic implants.

Key words: Bioceramic, Merwinite, Plasma spray coating.

Introduction

Bone injuries caused by trauma, tumor, and infection extremely affected people's daily life. Replacing bone substance can improve pain and renovate parts of body function. Thus, artificial orthopedic replacement implants have been developed in the past 30 years. Among them, titanium (Ti) and its alloys, Ti-6Al-4V have been widely utilized because of their superb mechanical properties, biocompatibility and corrosion resistance [1]. Nevertheless, their slow osseointegration and weak mechanical anchorage to host bone tissue limit the long-term clinical implantation. Several bioceramics such as, hydroxyapatite (HA) have been shown to directly bond with the bone tissue. However, the inadequate strength of bioactive ceramics hinder their application under load bearing situations [2] Plasma sprayed HA coatings have been used for orthopedic implants [3] However, HA coatings possess low osteogenic activity [4, 5] and relatively low bonding strength to Ti-6Al-4V substrate [6, 7] cause short-term osseointegration and low durability for long-term implantation. Therefore, a new kind of bioactive silicate bioceramics have attracted attention as biomedical coatings. Plasma sprayed calcium-silicate (Ca-Si) based coatings, including $CaSiO_3$ and Ca_2SiO_4 exhibited excellent bioactivity and short-term osseointegration and have been used for coating on Ti-6Al-4V[8-11] However, their poor chemical stability is the major problem weakens the long-term stability as orthopedic implants [12] Several Mg, Ca, Zn, Ti and Si-containing bioactive coatings such as, diopside ($CaMgSi_2O_6$) [10] sphene ($CaTiSiO_5$) [13] and hardystonite ($Ca_2ZnSi_2O_7$) [12] have been developed to improve the chemical stability of Ca-Si-based coatings. Thereby, it is important to select suitable bioactive ceramics to improve the osseointegration and bonding strength of orthopedic coatings on Ti alloys. Previously studies have shown that Ca-Si-Mg ceramics possessed bioactivity for stimulating bone regeneration [14, 15] Recently, plasma sprayed akermanite ($Ca_2MgSi_2O_7$) [16] and bredigite ($Ca_7MgSi_4O_{16}$) [17] have shown improved bonding strength as well as apatite formation and cytocompatibility on Ti-6Al-4V alloy compared to HA coating [16] Merwinite ($Ca_3MgSi_2O_8$) is another kind of Mg-containing bioactive compound. We have previously shown that merwinite ceramics possess the ability to induce apatite formation in simulated body fluids (SBF) [18, 19] Furthermore, it was shown that merwinite bioceramics support osteoblast cell (OB) adhesion and spreading [20] and L-929 fibroblast cells spreading [21] Also, in vivo evaluation of merwinite showed more and quick bone formation than HA. Previous studies have revealed that the merwinite ceramics exhibited excellent mechanical properties and biocompatibility [20] Also, The bending strength, Young's modulus and fracture toughness of merwinite ceramics were about 151 MPa, 31 GPa and 1.72 MPa $m^{1/2}$, respectively which was close to that of cortical bone (bending strength: 50-

*Corresponding author:
Tel : +982636280040
Fax: +982636280024
E-mail: mhafezi@merc.ac.ir

150 MPa; Young's modulus:7-30 GPa; 2-12 MPa $m^{1/2}$) [20] The CTE of the merwinite ceramic was close to the CTE of Ti-6Al-4V[20] Razavi et al have prepared merwinite coatings on Mg alloy using micro-arc oxidation (MAO) and electrophoretic deposition (EPD) technique that exhibited improved corrosion resistance and *in vitro* bioactivity [21, 22]

Materials and Method

Preparation of merwinite powders

Nanostructured-merwinite powders were synthesized by sol-gel method according to our previous study [19] After granulation, the obtained powders were sieved through 80 mesh.

Preparation of plasma-sprayed merwinite coatings

Ti-6Al-4V substrate with dimensions of 1 mm × 1.5 mm × 0.2 mm were ultrasonically grit blasted and then, washed with ethanol and dried at 60 °C before plasma spraying. An atmosphere plasma spray system (Sulzer Metco, Switzerland) was used to spray the synthesized powders onto the treated substrates. The detailed parameters for preparing plasma-sprayed coatings are shown in Table 1.

Characterization of prepared powders

The phase composition of the synthesized nanostructured-merwinite powders were determined by X-ray diffraction (XRD, Philips X'PERT MPD, Germany), using Cu Kα radiation at 40 kV and 40 mA (scan range: 10-70 °, step size: 0.02 °). The crystallite size of merwinite powder was determined using the Scherrer equation:

$$B = k\lambda/t\cos\theta \quad (1)$$

where λ is the wavelength (0.15406 nm), θ is the Bragg angle, k is a constant (0.9), and t is the apparent crystallite size. The morphology and microstructure of the merwinite powders were evaluated by scanning electron microscopy (SEM, Stereoscan S360, Cambridge, Germany) and transmission electron microscopy (TEM, GM200 PEG Philips, The Netherlands), respectively.

Characterization of prepared coatings

The morphologies and composition of coating's surface and cross section were observed by SEM with an energy-dispersive spectroscopy (EDS, XMD300, Germany) and atomic force microscopy (AFM, Tempe, AZ, USA). The coated samples were fixed in resin and sections were cut using a diamond saw (Exakt 300CL, Exakt Apparatebau, Germany) and subsequently ground and polished with an Exakt 400 CS Micro Grinding System (Exakt Apparatebau, Germany) before analyzing by SEM. The micro-hardness of the coatings was evaluated on the polished coating surfaces utilizing a micro-hardness tester (Akashi, MVK-H21, Japan) in accordance with ASTM-C1327-08 with a load of 300 gf and a loading time of 15 s.

Table 1. Plasma spraying parameters.

Gun Type	3MB Metco
Argon flow rate (SCFH)	85
Hydrogen gas flow rate (SCFH)	10
Current (A)	400
Voltage (V)	55
Argon powder carrier gas	10
Powder feed rate (Lbs./Hr.)	9
Spray distance (cm)	10

Results and Discussion

Characterization of the powder and coatings

XRD analysis shows that the crystal phase of the prepared powders is merwinite (JCPDS: 035-0591) with the crystal planes of (013), (411), (020), (600), (404), ($\bar{4}02$) and ($\bar{4}22$). Furthermore, the sharp peaks in the XRD pattern indicate the crystalline phase of merwinite powders after heat treatment as shown in Fig. 1. a According to Scherrer equation, the grain size of merwinite powders was about 30 nm. Also fig 1.b shows the main crystal phase of coating is merwinite (JCPDS:035-0591) with a small amount of amorphous

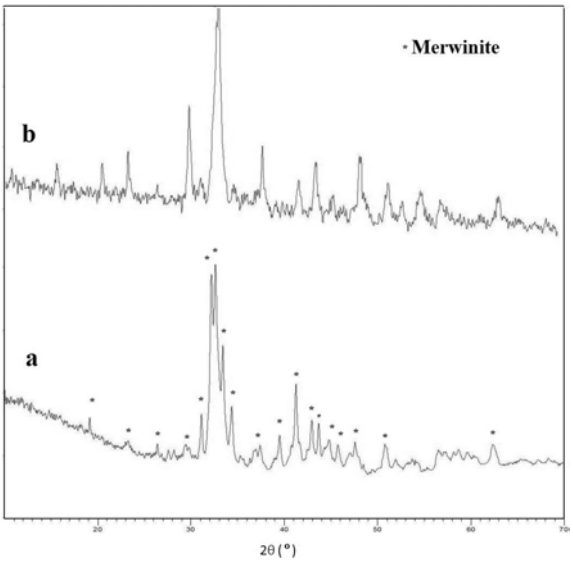

Fig. 1. XRD pattern of powder synthesized by sol-gel method after calcination at 900 C (a), and coating (b).

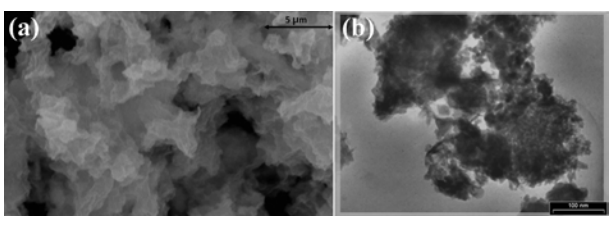

Fig. 2. The (a) SEM and (b) TEM of the synthesized merwinite powder.

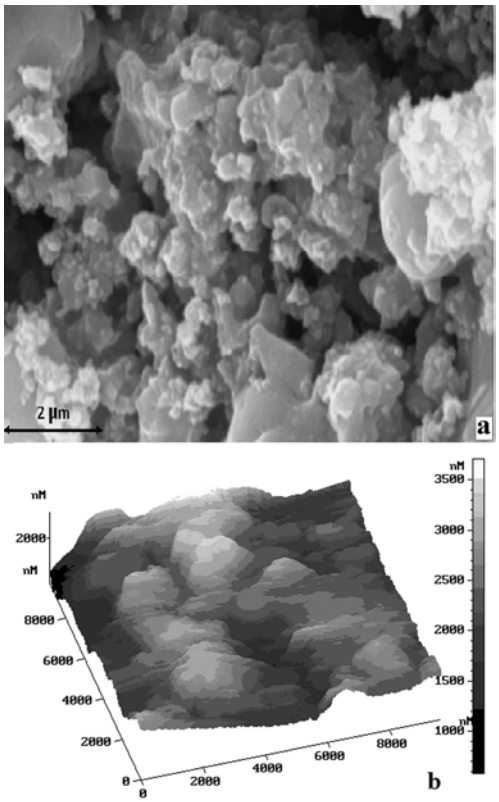

Fig. 3. Surface SEM (a) and (b) AFM analysis of merwinite coating.

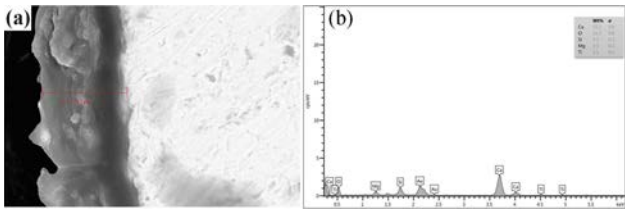

Fig. 4. Cross sectional (a) SEM and (b) EDX of merwinite coating.

phase. An amorphous phase is often observed in plasma sprayed ceramic coatings. Fig. 2 (a,b) shows the SEM (a) and TEM (b) of nanostructured merwinite that was synthesized by sol-gel method, respectively and indicates that the powders possess a nonhomogeneous structure and revealed agglomerative morphologies with irregular shape and the particle sizes were about 10-30 nm. Fig. 3 (a,b) shows the SEM and AFM analysis of coating, respectively which revealed that the merwinite coating is uniform and possess a particle size of less than 1 µm and a rough surface which was suitable to bone implants. The roughness of the merwinite coating is 0.252 ± 0.02 µm. Also, the Vickers hardness of merwinite coating was 177 ± 22.8 Hv. The polished cross-section of merwinite coating indicates that the coating thickness is about 16.4 µm (Fig. 4a). No microcracks was observed at the interface between substrate and coating which indicated good bonding between them. This can be attributed to the similarity of thermal expansion coefficients between merwinite coating and substrate. Also, no pores and micro cracks were observed in the coating. The EDX analysis of cross-section showed that Ca, Mg, Si and O elements are found in the structure of the coating (Fig. 4b).

In this study, we have successfully prepared plasma-sprayed merwinite coating on Ti-6Al-4V substrate. The plasma spraying method produced merwinite coating with denser microstructure due to better sintering properties compared with sol-gel method which were studied by other researchers. The surface characteristics of implants such as roughness affect the cell proliferation and attachment and the adsorption of proteins [23] indicating that the high surface roughness provide more area for biomaterial interactions. The bone cells are preferred to interact with rough surface [24] As can be seen, Ti-6Al-4V coated with merwinite possesses improved surface roughness than uncoated Ti alloy [24] which may have better biological properties [25] The plasma spraying, applies high deposition rates and produce dense microstructure, denser bonding interface and rough surface, which is suitable for bone substitutes [26, 9] The nanostructured merwinite coating has surface uniformity with a dense structure and low porosity. Thermal expansion coefficient (CTE) of ceramics is the other parameter influencing the bonding strength between the coatings and the substrate [27, 26, 9] Merwinite ceramics has a CTE of 9.87×10^{-6} /ºC which is similar to that of 9.80×10^{-6} /ºC for Ti-6Al-4V alloy [20] and thus, providing higher bonding strength and decrease the residual stress due to the mismatch of CTE. The cross-section area of merwinite coating has suitable uniformity with no microcracks as well as good integrity between the coating and underlying substrate compared to the plasma-sprayed akermanite coating exhibited longitudinal microcracks in the cross-section of coating due to the mismatch of CTE between coating and Ti alloy [16] The nanostructure of the merwinite coating is formed through unmelted particles surrounded in the melted main -body, which may contribute to improve the toughness and the wear resistance properties of the coating as well as a positive effect to its stability [28-30] In this study, the merwinite coating comprises mainly crystalline phase and a small amount of amorphous phase. The amorphous phase partially comes from the decomposition of $Ca_3Mg Si_2O_8$ during the high temperature plasma spraying process, which is frequently observed in plasma sprayed coatings [10] It is worth noting that the chemical composition and surface topography of the biomaterial can change the cellular responses. [31-34] The chemical composition of plasma-sprayed merwinite coating is significantly different than Ti alloy. Thus, it can be speculated that the difference between the chemical composition of coated Ti alloy and uncoated Ti plays a key role in the cellular response. In addition, previous studies have reported that ionic environment due to the dissolution of ions from biomaterials has an essential effect on the biological responses of cells [35, 36]

Differences in the composition of materials will lead to different ionic environments [37-39] The Ca, Si and Mg ions present in the structure of merwinite coating play an important role in stimulating cell proliferation and differentiation [38-41].

Conclusion

Nanostructured merwinite coatings were successfully prepared on Ti-6Al-4V by plasma spraying technique. The coating increased the surface roughness of substrate alloy. On the whole, according to the results, plasma-sprayed merwinite coating on Ti-6Al-4V may be a good candidate for orthopedic applications. However, in vitro and in vivo evaluation of coating is necessary.

Acknowledgments

The authors would like to acknowledge the Iran National Science Foundation (INSF) for the financial support of this work, through grant No. 93022644.

References

1. Q. Fu, Y. Hong, et al., Biomaterials 32 [30] (2011) 7333-7346.
2. X. Zheng, M. Huang, et al., Biomaterials 21 [8] (2000) 841-849.
3. M. Nagano, T. Nakamura, et al., Biomaterials 17 [18] (1996) 1771-1777.
4. L.L. Hench, Journal of the American Ceramic Society 74 [7] (1991) 1487-1510.
5. H. Oonishi, L. Hench, et al., Journal of biomedical materials research 44 [1] (1999) 31-43.
6. R. McPherson, N. Gane, et al., Journal of Materials Science: Materials in Medicine 6 [6] (1995) 327-334.
7. K. Khor, C. Yip, et al., Journal of thermal spray technology 6 [1] (1997) 109-115.
8. X. Liu, S. Tao, et al., Biomaterials 23 [3] (2002) 963-968.
9. X. Liu, C. Ding, et al., Biomaterials 25 [10] (2004) 1755-1761.
10. W. Xue, X. Liu, et al., Surface and Coatings Technology 185 [2] (2004) 340-345.
11. W. Xue, X. Liu, et al., Biomaterials 26 [17] (2005) 3455-3460.
12. K. Li, J. Yu, et al., Journal of Materials Science: Materials in Medicine 22 [12] (2011) 2781-2789.
13. C. Wu, Y. Ramaswamy, et al., Journal of The Royal Society Interface 6 [31] (2009) 159-168.
14. Y. Huang, X. Jin, et al., Biomaterials 30 [28] (2009) 5041-5048.
15. L. Xia, Z. Zhang, et al., Eur Cell Mater 22 (2011) 68-82.
16. D. Yi, C. Wu, et al., Biomedical Materials 7 [6] (2012) 065004.
17. D. Yi, C. Wu, et al., J Biomater Appl (2013).
18. M. Hafezi-Ardakani, F. Moztarzadeh, et al., Journal of Ceramic Processing Research 11 [6] (2010) 765-768.
19. M. Hafezi-Ardakani, F. Moztarzadeh, et al., Ceramics International 37 [1] (2011) 175-180.
20. J. Ou, Y. Kang, et al., Biomed Mater 3 [1] (2008) 015015.
21. M.Razavi, M.Fathi et al, Ceramics International, 40 [7] (2014) 9473-9484.
22. M. Razavi, M. Fathi, et al., Surface and Interface Analysis 46 [6] (2014) 387-392.
23. S.R. Paital and N.B. Dahotre, Materials Science and Engineering: R: Reports 66 [1] (2009) 1-70.
24. C. Wu, Y. Ramaswamy, et al., Acta biomaterialia 4 [3] (2008) 569-576.
25. E. Gyorgy, S. Grigorescu, et al., Applied surface science 253 [19] (2007) 7981-7986.
26. X. Liu, P.K. Chu, et al., Materials Science and Engineering: R: Reports 47 [3] (2004) 49-121.
27. E. Saiz, M. Goldman, et al., Biomaterials 23 [17] (2002) 3749-3756.
28. E.H. Jordan, M. Gell, et al., Materials Science and Engineering: A 301 [1] (2001) 80-89.
29. X.-Q. Zhao, H.-D. Zhou, et al., Materials Science and Engineering: A 431 [1] (2006) 290-297.
30. H. Chen, G. Gou, et al., Surface and Coatings Technology 203 [13] (2009) 1785-1789.
31. H. Zreiqat, C. Howlett, et al., Journal of biomedical materials research 62 [2] (2002) 175-184.
32. H. Zreiqat, S.M. Valenzuela, et al., Biomaterials 26 [36] (2005) 7579-7586.
33. X. Liu, J.Y. Lim, et al., Biomaterials 28 [31] (2007) 4535-4550.
34. S. Heo, D. Kim, et al., Journal of the Royal Society Interface 5 [23] (2008) 617-630.
35. P. Valerio, M.M. Pereira, et al., Biomaterials 25 [15] (2004) 2941-2948.
36. C. Wu, J. Chang, et al., Biomaterials 26 [16] (2005) 2925-2931.
37. C. Wu, J. Chang, et al., Journal of Biomedical Materials Research Part A 76 [1] (2006) 73-80.
38. C. Wu, J. Chang, et al., Journal of Materials Science: Materials in Medicine 18 [5] (2007) 857-864.
39. C. Wu, Y. Ramaswamy, et al., Biomaterials 28 [21] (2007) 3171-3181.
40. I.A. Silver, J. Deas, et al., Biomaterials 22 [2] (2001) 175-185.
41. C. Wu and J. Chang, Journal of biomaterials applications 21 [3] (2007) 251-263.